Nonlinear Collisionless Magnetic Reconnection

M. Ottaviani and F. Porcelli
JET Joint Undertaking, Abingdon, Oxfordshire, OX14 3EA, United Kingdom
(Received 30 August 1993)

Collisionless magnetic reconnection in regimes where the mode structure is characterized by global convection cells is found to exhibit a quasiexplosive time behavior in the early nonlinear stage where the fluid displacement is smaller than the equilibrium scale length. This process is accompanied by the formation of a current density sublayer narrower than the skin depth. This sublayer keeps shrinking with time.

PACS numbers: 52.35.Py

Magnetic reconnection in collisionless regimes, where electron inertia is responsible for the decoupling of the plasma motion from that of the magnetic field, is a well known process in astrophysics [1]. It is quite exciting that this process can now be observed in laboratory plasmas produced by tokamaks such as the Joint European Torus (JET). Indeed, at the high plasma temperatures of these experiments, internal plasma relaxations (the so-called [2] *sawteeth*) can occur on a time scale shorter than the electron-ion collision time. Motivated by these observations, the linear theory of $m=1$ kink-tearing modes, which trigger the sawtooth relaxations, has recently been extended to experimentally relevant regimes [3–6], leading to the conclusion that these modes can remain virulent at low collisionality with an initial growth rate which compares favorably with that observed in the experiments. However, the nonlinear evolution has remained unclear. While Wesson's [7] modification of the Sweet-Parker-Kadomtsev [8–10] scaling has given an estimate of the collisionless reconnection time in good agreement with that observed experimentally, Drake and Kleva's numerical simulation [11] of the merging of two isolated flux bundles has led to the suggestion that the collisionless reconnection rate is greatly reduced as the nonlinear phase is entered, i.e., for magnetic island widths comparable with the plasma skin depth. Later investigations taking into account the finite ion (sound) Larmor radius found exponential [12] or even faster [13] nonlinear growth.

With the aim of clarifying these issues, we present the numerical and analytic solution of a collisionless, incompressible, 2D slab model where Larmor radius effects are neglected. The equations we solve are

$$\partial_t U + [\varphi, U] = [J, \psi] , \tag{1}$$

$$\partial_t F + [\varphi, F] = 0 , \tag{2}$$

where we use the notation $\partial_t \equiv \partial/\partial t$ and

$$[A,B] \equiv \mathbf{e}_z \cdot \nabla A \times \nabla B ,$$

with $\mathbf{e}_z$ the unit vector along the z direction. $U = \nabla^2 \varphi$ is the fluid vorticity, φ is the stream function, $\mathbf{v} = \mathbf{e}_z \times \nabla \varphi$ is the fluid velocity, $J = -\nabla^2 \psi$ is the current density along z, ψ is the magnetic flux function, and $F \equiv \psi + d^2 J$ is the canonical momentum along the field lines, with d the inertial skin depth. Thus, $[\varphi, F] = \mathbf{v} \cdot \nabla F$ and the collisionless Ohm law (2) can be written as $dF/dt = 0$; i.e., F is conserved on a moving fluid element. The coordinate z is ignorable, $\partial_z = 0$. The coordinates x and y vary in the intervals $x \in [-L_x, L_x]$ and $y \in [-L_y, L_y]$, with the slab aspect ratio $\varepsilon \equiv L_x/L_y < 1$. Periodic boundary conditions are imposed at the edge of these intervals. The magnetic field is $\mathbf{B} = B_0 \mathbf{e}_z + \nabla \psi \times \mathbf{e}_z$, with B_0 a constant value which we take to scale as $B_0 \sim \varepsilon^{-1} |\nabla \psi|$ in order to mimic the magnetic field of a tokamak. All quantities in Eqs. (1) and (2) are dimensionless, with L_x and $\tau_A = (4\pi \rho_m)^{1/2} \times L_x/B_y$ determining the length and time scale normalization.

We consider an equilibrium specified by $L_x = \pi$, $\varphi_0 = U_0 = 0$, $J_0 = \psi_0 = \cos x$, and $F_0 = (1 + d^2)\psi_0$. This equilibrium is tearing unstable to linear perturbations of the type $(\varphi, \delta\psi) = \mathrm{Re}\{[\varphi_L(x), \delta\psi_L(x)] e^{\gamma t + iky}\}$, with $k = m\varepsilon$ and m an integer number, and with $\varphi_L(x)$ and $\delta\psi_L(x)$ respectively odd and even functions around the two equivalent reconnecting surfaces at $x = 0$ and at $x = \pm L_x$. In the limit $d \ll L_x$, the solution of the linearized system can be obtained analytically using asymptotic matching techniques. Electron inertia is important within narrow layers around the reconnecting surfaces. In the *outer* region, the linearized mode structure for $0 < k^2 \leq 1$ is $\delta\psi_L = \psi_\infty \cos[\kappa(|x| - \pi/2)]$ and $\varphi_L = (i\gamma/k \sin x)\delta\psi_L$, with ψ_∞ a constant and $\kappa \equiv (1 - k^2)^{1/2}$. Instability requires that the outer region parameter $\Delta' \equiv |d \ln \delta\psi_L / dx|_{x=0^-}^{x=0^+}$ be positive. In our case, $\Delta' = 2\kappa \tan(\kappa\pi/2)$. We consider the *large*-Δ' regime, defined by

$$\Delta' d \geq 1 , \tag{3}$$

which can be satisfied for low values of m and $\varepsilon^2 \ll 1$ such that $\Delta' \sim 8/\pi k^2$. In this regime, the structure of the stream function is macroscopic, with $\varphi_L \approx \varphi_\infty \mathrm{sgn} x$, $\varphi_\infty \equiv (i\gamma/k)\psi_\infty$, everywhere except in the reconnection layers. For $\Delta' d \gg 1$, the eigenfunctions in the vicinity of the layer at $x = 0$ take the form $\delta J_L \approx -\psi_\infty (2/\pi d^2)^{1/2} \times \exp(-x^2/2d^2)$ and $\varphi_L \approx \varphi_\infty \mathrm{erf}(x/2^{1/2}d)$, which match onto the outer solution for $|x| > d$. Thus, the current layer in the linear stage has a width $\delta_L \sim d$. The linear

0031-9007/93/71(23)/3802(4)$06.00

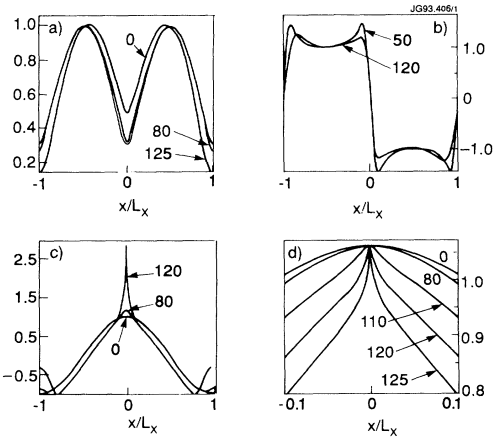

FIG. 1. Cross sections of (a) $\delta\psi/(\delta\psi)_{x=L_x/2}$; (b) $v_x/(v_x)_{x=-L_x/2}$; (c) J; (d) F versus x at $y=0$. The X point is at $x=0$; the O point of the second island chain is at $x=\pm L_x$. Times are indicated by the arrows.

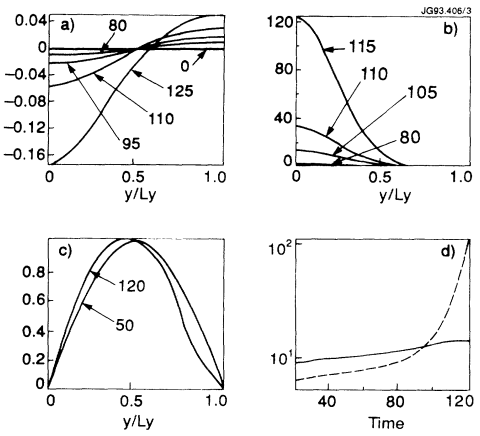

FIG. 2. Cross sections of (a) $\delta\psi$; (b) $\partial^2 F/\partial x^2$; (c) $v_y/(v_y)_{y=L_y/2}$ versus y at $x=0$. The island's X and O points are at $y=0$ and $y=L_y$, respectively. Also, (d) time dependence of the logarithm of the inverse scale lengths δ_φ^{-1} (solid line) and δ_J^{-1} (broken line).

growth rate is $\gamma_L \approx kd$.

The system of Eqs. (1) and (2) is solved numerically with a pseudospectral code [14] which advances in time the Fourier representation of the field variables, truncated to 1024×64 (x,y) components. We are interested in the early nonlinear phase, defined by the condition $d<w<2L_x$, where w is the magnetic island width. The initial conditions are chosen to approximate closely the linear eigenfunctions, and in particular to reproduce the spatial symmetries of the linear solution around the X and O points and the reflection symmetry with respect to the four points $x=\pm L_x/2$, $y=\pm L_y/2$. It can be easily verified by inspection of (1) and (2) that these symmetries are preserved during the nonlinear evolution. An important consequence is that the value of F at $x=0$ is frozen to its initial value, i.e., $F(x=0,y,t)=F_0(x=0)=1+d^2$.

For $\varepsilon\ll1$, the adopted equilibrium is linearly unstable to several mode numbers, m. On the other hand, in the numerical analysis of the full nonlinear system (1) and (2), it is convenient to follow the evolution of a single linearly unstable mode. This requirement is dictated both by reasons of simplicity and by analogy with the kink-tearing instability in a toroidal plasma. Therefore, we present numerical runs with $\varepsilon=0.5$ and $d/2L_x=0.04$, which give $d\Delta'\approx2.03$ for $m=1$, thus satisfying the large-Δ' condition (3), while the other m values are stable ($\Delta'\le0$ for $m\ge2$). Figure 1 shows sections of $\delta\psi\equiv\psi-\psi_0$, $v_x=-\partial\varphi/\partial y$, J and F across the X point ($y=0$) at various times. The linear phase conventionally lasts until $t\sim80$, when the magnetic island reaches a width of order d. The linear layer width $\sim d$ is visible from these graphs. For $t>80$, the width of the profile of v_x, $\delta_\varphi\equiv(v_x)_{x=L_x/2}/(\partial_x v_x)_{x=0}$, as well as that of $\delta\psi$, remain of the order of the skin depth [Figs. 1(a) and 1(b)]. By contrast, the current density profile [Fig. 1(c)] develops a sublayer whose width around the X point, $\delta_J\equiv(\partial_x^2\delta J/\delta J)^{-1/2}<d$, keeps shrinking with time [see also Fig. 2(d)]. Here, $\delta J\equiv J-J_0$. This sublayer is also visible in the profile of F across the X point [Fig. 1(d)]. The contraction of this sublayer is extremely rapid in time, as shown by the graph of $\partial^2F/\partial x^2$ versus y for $x=0$ and several times in Fig. 2(b). At $t\approx125$, it has become so narrow that it can no longer be resolved by our truncated Fourier expansion, and so the simulation is stopped. Also shown in Figs. 2(a) and 2(c) are the profiles of $\delta\psi$ and of $v_y=\partial\varphi/\partial x$ along the reconnection line ($x=0$) at various times, from which it is clear that only a limited number of Fourier harmonics along y are involved in the early nonlinear evolution. Contour plots of φ, ψ, J, and F are shown in Fig. 3. Note that the convection cells retain approximately their linear shape well into the nonlinear phase [Fig. 3(a)]. Also note the development of a current sheet around the reconnection line [Fig. 3(c)] and the preservation of the topology of the isolines of F [Fig. 3(d)]. Finally, Fig. 4 summarizes the time behavior. It is remarkable that the mode growth remains very rapid throughout the simulation. Indeed, the growth of φ, as well as that of $\delta\psi$ and δJ at the X points, accelerates in the early nonlinear phase, which is symptomatic of an explosive behavior. However, the mode growth slows down when w approaches L_x, as we have observed in a simulation with $d/2L_x=0.08$ (not shown here).

The fact that the spatial structure of the stream function does not vary significantly with time throughout the linear and early nonlinear phases suggests the ansatz

$$\varphi(x,y,t)=v_0(t)g(x)h(y)+u(x,y,t)\,, \tag{4}$$

where $h(y)\sim k^{-1}\sin(ky)$, $g(x)\sim\varphi_L(x)/\varphi_\infty$ contains the linear scale length d and $u(x,y,t)$ develops the rapid scale length $\delta(t)\sim\delta_J$ observed in the numerical simula-

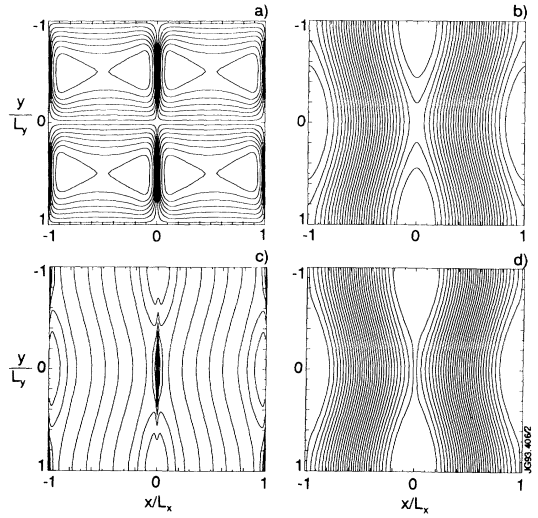

FIG. 3. Contour plots at $t=120$: (a) φ; (b) ψ; (c) J; (d) F.

tion. We assume $u \ll v_0$ and $\partial_x u \sim v_0 \partial_x g$, which is consistent with the near constancy in time of the width of v_x across the reconnecting layer [Fig. 2(d)], as well as that of the ratio $v_y(0,L_y/2,t)/v_x(-L_x/2,0,t)$ (Fig. 4). These assumptions allow an analytic treatment of the system of Eqs. (1) and (2).

The collisionless Ohm law (2) can be integrated exactly to yield $F=F_0(x_0)$, where $x_0(x,y,t)=x-\xi(x,y,t)$ is the initial position of a fluid element situated at (x,y) at time t and ξ is the displacement along the x direction defined by the equation $d\xi/dt=v_x$, $\xi(t=-\infty)=0$. The latter equation can be integrated using the methods of the characteristics. At $y=0$, where v_y vanishes, using the ansatz (4) where $u(x,y,t)$ can be neglected, we find

$$-\int_{x_0}^{x} dx'/g(x') = \int_{-\infty}^{t} v_0(t')dt' \equiv \lambda(t) . \tag{5}$$

The function $\lambda(t)>0$ represents the amplitude of ξ outside the reconnection layer, where $g(x)\approx 1$. In the linear phase, $-\psi_\infty \approx \lambda < d$. When $\lambda > d$, the magnetic island width $w \sim 2\lambda$, so that the early nonlinear phase can also be characterized by the inequality $d<\lambda<L_x$, or alternatively $t_0<t<t_D$, with $\lambda(t_0)\sim d$ and t_D the characteristic turnover time of the macroscopic eddies in Fig. 3(a).

Equation (5) can be inverted to obtain $x_0=x_0(x,t)$. Again, we use the ansatz (4), in particular the assumptions $\hat{d} \equiv (dg/dx)_{x=0}^{-1} \sim d$ and $g \to 1$ for $x > d$. In the limit $d<\lambda<L_x$, the time-dependent scale length is found,

$$\delta(t) \equiv \hat{d} \exp[-\lambda(t)/\hat{d}] , \tag{6}$$

such that x_0 has the following behavior around $y=0$: $x_0 \sim (x/\delta)\hat{d}$ for $|x|<\delta$; $x_0 \sim [\lambda+\hat{d}\ln(|x|/\hat{d})]\,\mathrm{sgn}(x)$ for $d>|x|>\delta$; and $x_0 \sim \lambda\,\mathrm{sgn}(x)+x$ for $|x|>d$. Thus we see that near the X point along the x direction, $F(x_0)$ (and hence J) varies over a distance $\delta(t)$ which becomes exponentially small in the ratio $\lambda/\hat{d}$. Conversely, around $y=\pm L_y$, $\lambda \to -\lambda$ in Eq. (5). Then, $x_0<d$ for $|x|<\lambda$ and F flattens over a distance $|x| \sim \lambda$ from the O point. We stress that the formation of a sublayer is the combined result of the conservation of F on each fluid element and the flow pattern around the X point, which acts to increase the local curvature of the F profile [Fig. 1(d)].

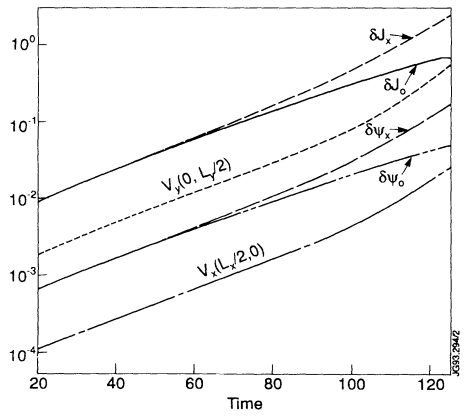

FIG. 4. Time dependence of $\delta\psi$ and δJ at the X and O points, of $v_x(-L_x/2,0)$ and of $v_y(0,L_y/2)$.

Next, we obtain an expression for ψ by integrating the equation $\psi+d^2J=F$, where we can approximate $J \approx -\partial_x^2\psi$. Using as asymptotic boundary condition the matching of $\delta\psi$ to the linear solution for $\lambda<|x|<L_x$, we obtain $\psi(x,y,t) \approx \frac{1}{2}\int_{-\infty}^{\infty} e^{-|\hat{x}-\hat{x}'|}F(\hat{x}',y,t)d\hat{x}'$, where $\hat{x} \equiv x/d$, which shows that ψ has an integral structure such that any fine scale variation of F is smoothed out over a distance $\sim d$. Asymptotic evaluation of ψ at the X and O points in the early nonlinear phase gives

$$\begin{aligned} &\psi_X \equiv \psi(0,0,t) \sim 1-\tfrac{1}{2}\lambda^2(t) , \\ &\psi_O \equiv \psi(0,\pm L_y,t) \sim 1+\mathcal{O}(d^2) . \end{aligned} \tag{7}$$

Let us set $F=F_0(x)+\delta F$. Then, $\delta\psi+d^2\delta J=\delta F$, and at $x=0$, where $\delta F=0$, we find $\delta J=-\delta\psi/d^2$. Thus we have demonstrated that an asymmetry develops in the values of $\delta\psi$ and of J between the X and O points. The spike of the current density at the X point has an amplitude $\delta J_x \sim 0.5(\lambda/d)^2$.

Let us now integrate the vorticity equation (1) over the quadrant $S:[0\le x\le L_x, 0\le y\le L_y]$, such that $\int_S [\varphi,U] \times dx\,dy=0$. Using Stokes' theorem, we obtain

$$\partial_t \int_S U dx\,dy = \oint_C J\,d\psi , \tag{8}$$

where C is the boundary of S. With the ansatz (4), and neglecting corrections $\mathcal{O}(\varepsilon k d)$ contributed by $\partial_y^2\varphi$, we find

$$\partial_t \int_S (\partial_x^2\varphi)dx\,dy \approx -(4c_0c_1/k^2d)d^2\lambda/dt^2 , \tag{9}$$

where $c_0 \equiv d/\hat{d}$ and $c_1(t) = 1 + (d/c_0 v_0)(\partial_x u)_X$ is a factor of order unity, which depends weakly on time [e.g., $1 \leq c_1 \leq 1.4$ in Fig. 2(d)]. Exploiting the reflection symmetry with respect to $x = L_x/2$, $y = L_y/2$, the second integral in Eq. (8) can be written as

$$\oint_C J\, d\psi = -2\int_0^{L_y} dy\,(J\partial_y\psi)_{x=0} - 2\int_0^{L_x} dx\,[(\partial_y^2\psi)(\partial_x\psi)]_{y=0}.$$

The first integral on the right hand side (r.h.s.) can be evaluated exactly:

$$-\int_0^{L_y} dy\,(J\partial_y\psi)_{x=0} = \delta\psi_X - \delta\psi_O - (\delta\psi_X^2 - \delta\psi_O^2)/2d^2. \tag{10}$$

The second integral gives a contribution of order $k^2\lambda$, which is negligible when $\Delta' d \sim 8d/\pi k^2 > 1$, and which is significant only in the linear phase when $\Delta' d \sim 1$.

Interpolating between the leading linear and early nonlinear behaviors of the r.h.s. of (10) [i.e., $-(8/\pi)^{1/2}\lambda d$ and $-\lambda^4/8d^2$, respectively], and inserting this and (9) into (8), we obtain an equation for the evolution of $\hat{\lambda}(t) \equiv \lambda(t)/d$:

$$d^2\hat{\lambda}/d\hat{t}^2 \approx \hat{\lambda} + c_2\hat{\lambda}^4, \tag{11}$$

where $\hat{t} \equiv \gamma_L t$ and $c_2 \approx 1/16 c_0 c_1 > 0$ can be taken constant. The solution is $\hat{\lambda}(\hat{t}) = [(1-\alpha)/(1-\alpha e^{3\hat{t}})]^{2/3} e^{\hat{t}}$, where $\alpha = \beta - (\beta^2 - 1)^{1/2}$, $\beta = 1 + 5/c_2$, and we have chosen the time origin so that $\hat{\lambda}(0) \equiv 1$. Thus, once the early nonlinear regime is entered, $\lambda(t)$ accelerates and reaches a macroscopic size over a time, $t_c \sim \ln(\alpha^{-1/3})\gamma_L^{-1}$, of the order of the linear growth time. As we remarked earlier, we can expect this quasiexplosive growth to cease as λ approaches L_x.

In conclusion, collisionless reconnection in regimes where the instability parameter Δ' is large and macroscopic convection cells develop does not follow the standard Sweet-Parker scenario [8,9]. In these regimes, we find an early nonlinear phase, characterized by a magnetic island larger than the skin depth but smaller than the size of the convection cells, during which reconnection proceeds faster than exponentially. Physically, the flow rotation accelerates following the intensification of the electromagnetic torque $\oint_C \mathbf{J}\times\mathbf{B}\cdot d\mathbf{l} = \oint_C J\, d\psi$ during the early nonlinear phase. This torque is mainly contributed by the average $J_z B_x$ force between the X and O points within a magnetic island, corresponding to the integral of Eq. (10). The formation of a current spike narrower than the skin depth, already noted in Ref. [11], is here found to be the consequence of the conservation of the parallel canonical momentum on moving fluid elements and the flow pattern around the X point. The different conclusion of Ref. [11], i.e., that reconnection slows down in the nonlinear regime, may be due to a ratio of the skin depth to the macroscopic scale length close to unity used there. Indeed, a suitable separation between the skin depth and the macroscopic scales is needed to explore the early nonlinear phase. The spike formation was also conjectured in Ref. [7], although its consequences on the reconnection dynamics were not worked out.

As an extremely narrow current spike develops during the reconnection process, the electron distribution function tends to become highly distorted and one can think of instabilities which would limit this tendency, introducing an effective ("anomalous") current diffusion. Clearly, a refined model is needed to describe this for realistic experimental parameters, with effects such as the finite ion Larmor radius, density and pressure gradients, 3D, etc., likely to play an important role. Nevertheless, we believe that the present analysis opens the possibility to understand the rapidity of relaxation processes observed in low collisionality plasmas.

The authors would like to thank J. Wesson for stimulating discussions, and S. Migliuolo and F. Waelbroeck for useful comments.

[1] V. M. Vasyliunas, Rev. Geophys. Space Phys. **13**, 303 (1975).
[2] A. W. Edwards *et al.*, Phys. Rev. Lett. **57**, 210 (1986).
[3] F. Porcelli, Phys. Rev. Lett. **66**, 425 (1991).
[4] H. L. Berk, S. M. Mahajan, and Y. Z. Zhang, Phys. Fluids B **3**, 351 (1991).
[5] B. Coppi and P. Detragiache, Phys. Lett. A **168**, 59 (1992).
[6] L. E. Zakharov and B. Rogers, Phys. Fluids B **4**, 3285 (1992).
[7] J. Wesson, Nucl. Fusion **30**, 2545 (1990).
[8] P. A. Sweet, in *Electromagnetic Phenomena in Cosmic Physics*, edited by B. Lehnert (Cambridge Univ. Press, Cambridge, 1958), p. 123.
[9] E. N. Parker, J. Geophys. Res. **62**, 509 (1957).
[10] B. B. Kadomtsev, Fiz. Plasmy **1**, 710 (1975) [Sov. J. Plasma Phys. **1**, 389 (1975)].
[11] J. F. Drake and R. G. Kleva, Phys. Rev. Lett. **66**, 1458 (1991).
[12] L. E. Zakharov, B. Rogers, and S. Migliuolo, Phys. Fluids B **5**, 2498 (1993).
[13] A. Y. Aydemir, Phys. Fluids B **4**, 3469 (1992).
[14] S. A. Orszag and G. S. Patterson, Phys. Rev. Lett. **28**, 76 (1972).